NASA-116

Effects of Different Field Expansions

on

Omnidirectional Proton Counting Rate Data

by

S. E. DeForest

Department of Physics

University of California, San Diego

La Jolla, California

December, 1965

Investigations have been made at the Space Sciences Laboratory at the University of California, San Diego (UCSD) to determine the effects of improved expansions of the earth's magnetic field on data that have already been reduced using the previous 49-term expansion. Two new expansions have been used, the Jensen and Cain, (1964) expansion of 64 terms and the more recent 100 term one. (Cain, et al, 1965, Hendricks and Cain, 1966). The differences in the magnitude of B using the different expansions are small for the most part. Some direct comparisons are seen in Table 1.

Table 1

Effects of Different Field Expansions

Long.	Lat.	B^*_{49}	B_{64}	B_{100}	$100(B_{49}-B_{64})/B_{49}$	$100(B_{49}-B_{100})/B_{49}$
0	-30.	.58222	.52500	.52614	0.4008	0.1836
0	-10.	.57397	.57077	.57182	0.5598	0.3756
0	0.	.56139	.55809	.55875	0.5900	0.4726
0	+10.	.53778	.53548	.53598	0.4303	0.3370
0	+30.	.49308	.49352	.49327	-0.0894	-0.0377

$^*B_N$ = B calculated from N - term expansion.

At some locations, the percent difference is 2-3%. However, this does not give an indication of the effect of the field changes on the counting rate distribution in B-L space (McIlwain, 1961) for charged particles. Three methods can be used to demonstrate the effects:

1. An effective change in B can be defined which reflects the changes in counting rates to be expected at a given location in B-L space.

2. New counting rates can be computed at given points in space at which rates based on the old expansion are known. These two rates can then be compared directly.

3. Actual data points can be used to re-calculate B and L. These points can then be analyzed in the same manner as the original data.

The first two approaches have the advantage of producing curves which show the expected changes as functions of position, but they do not give any idea of the effect on the scatter of data from fitted curves. Therefore, an analysis of type (3) must also be conducted since this last result is an important direct measure of the value of using a particular field expansion.

Certain constants are needed for use with the first two techniques. To compute these, omnidirectional counting rates from Relay II were fitted to a least squares curve for several values of the magnetic parameter L. From these curves, the partial derivatives of the logarithm of the counting rate with respect to both B and L were found.

1. For a given set of geographic points, B and L were calculated using first the old expansion and then the newest (100-terms) one. Counting rates were found for these B, L coordinates from the least squares curves, and an effective Δ B was defined as

$$\Delta B_{eff} = \text{Log} \left(\frac{J_{49}}{J_{100}} \right) \bigg/ \left(\frac{\partial \text{ Log } \left(J_{49} / \left[1 \text{ per second} \right] \right)}{\partial B} \right)$$

and this was plotted against longitude for various ratios of B/B_o (B_o is the minimum value of B on a given line of force). The results for L = 1.6 appears in Figure 1. The effective Δ B was, on the average, 2-4 times greater than the actual change in B.

2. For the next comparison, a new counting rate was defined as

$$J_n = J_{49} \exp \left[(B_{49} - B_N) \frac{\partial \text{Log } (J)}{\partial B} + (L_{49} - L_N) \frac{\partial \text{Log } J}{\partial L} \right].$$

where J_n = counting rates for N-Term expansion

This represents the predicted counting rate for the same position using the new expansion. Then the quantity

$$\% \, \Delta J = (J_{49} - J_n) \times 100 / J_n$$

was plotted against longitude for several values of B/B_o and L = 1.6. The results are shown in Figure 2 for the cases where N is 64 and 100. For the ratios of B/B_o much greater than 2, the % Δ J increases rapidly, but the actual values of the counting rates also decreases rapidly, and the least squares fit upon which the analysis is based, becomes less accurate.

3. As can be seen from Figure 2, the fractional changes are approximately $\pm$ (1-2)% for both cases. If these changes are in fact due to errors in the old 49 term field then a significant reduction in the scatter of data should result from the use of the newer field representations. A great deal of computer time would be required to recalculate B and L for all points in a given region from the satellite. Instead, the points that have been interpolated to standard values of L are used as these form a much smaller set. The new values of B are kept with the interpolated values of L and a new counting rate defined as

$$J_n = J_{49} \exp \left[\Delta L \frac{\partial \operatorname{Log} (J)}{\partial L} \right]$$

This type of correction for the changes in L should be sufficient for the small changes expected from Figure 2. These corrections were made on Relay II omnidirectional data for both the 64 and 100-term expansions. The corrected points were then fitted to least square curves as before. The R.M.S. deviation from these curves are given in Table 2. Two values of L and two ranges of B were analyzed. As might have been predicted from Figure 2, the difference between the results due to the two improved expansions is much less than the difference between either one and the uncorrected data. It is also seen that the correction lowers the scatter considerably as long as the ratio of B/B_o considered is not much greater than about 3.5. For the case where this was violated ($L = 2.0$, $B/B_o = 3.60 - 5.14$), the scatter actually increased. This is probably due to two causes. The partial derivative with respect to L is not known accurately in this region. And the fractional change due to the change in the field is probably too large to justify the simple correction that was used. In that region it may be necessary to recalculate B-L from the original data before interpolation.

Table 2

Analysis of Corrected Relay II Data

Expansion	L	B^*_{MIN}	B_{MAX}	B_{MIN}/B_O	B_{MAX}/B_O	No. of points	R.M.S. Error	Aver. Error
49	1.6	.076	.15	1.0	1.97	184	4.07	3.09
64	1.6	.076	.15	1.0	1.97	186	3.01	2.25
100	1.6	.076	.15	1.0	1.97	186	2.97	2.22
49	2.0	.039	.15	1.0	3.85	262	4.55	3.44
64	2.0	.039	.15	1.0	3.85	263	3.94	2.95
106	2.0	.039	.15	1.0	3.85	263	3.93	2.94
49	1.6	.14	.20	1.84	2.52	29	3.71	2.80
64	1.6	.14	.20	1.84	2.52	28	2.71	2.10
100	1.6	.14	.20	1.84	2.52	28	2.68	2.09
49	2.0	.14	.20	3.60	5.14	88	5.45	4.46
64	2.0	.14	.20	3.60	5.14	86	6.48	5.10
100	2.0	.14	.20	3.60	5.14	86	6.30	5.01

*B in gauss

The decrease in scatter is actually more than it seems. If σ_T is the total scatter, and σ_F is the scatter due to errors in the field, and σ_0 is the scatter due to all other effects, then

$$\sigma_T^2 \cong \sigma_F^2 + \sigma_0^2$$

If it is assumed that the 100-term expansion completely removes σ_F then for the first case (L = 1.6, Low B)

$$\sigma_0^2 \approx 9$$

and

$$\sigma_T^2 \approx \sigma_F^2 + 9 \approx 16.$$

This gives

$$\sigma_F \approx 2.2\%$$

as the total error that has been removed.

It can be seen from Figure 2 that this is indeed the approximate decrease in scatter that would be expected if the differences in the fields were in fact primarily due to errors in the 49 term field. The scatter using the 64 and 100 term fields is not inconsistent with that expected from causes other than magnetic field errors. It is therefore not possible to estimate the scatter which can be attributed to the errors in the 64 and 100 term fields.

Figure 3 shows how the counting rate varies with magnetic field for the first two ranges considered in Table 2. These curves were plotted using the 49-term expansion.

Figure 4 shows an enlarged view of the segment of the curve for $L = 1.6$ that is enclosed in the rectangle. Also shown are the points as obtained using the 49-term expansion and the 100-term expansion.

In conclusion, it can be seen that a significant reduction in the scatter of trapped particle data can be obtained by the use of the newer field representations.

Acknowledgments

I thank Professor C. E. McIlwain for helpful discussion and advice during the course of this work. The work was supported in part by the National Aeronautics and Space Administration Contract NASr-116.

Figure Captions

Figure 1. Effective change in magnetic field versus longitude.

Figure 2. Predicted change in counting rate versus longitude.

Figure 3. Counting rate versus magnetic field.

Figure 4. Counting rate versus magnetic field with scatter of data shown.

References

Cain, J. C., W. E. Daniels, Shirley J. Hendricks, and Duane C. Jensen, An evaluation of the main geomagnetic field, 1940-1962, J. Geophys. Res., 70, 3647-3674, 1965.

Hendricks, S. J., and J. C. Cain, Magnetic field data for trapped-particle evaluation, J. Geophys. Res., 77, 346-347, 1966.

McIlwain, C. E., Coordinates for mapping the distribution of magnetically trapped particles, J. Geophys. Res., 66, 3681-3691, 1961.

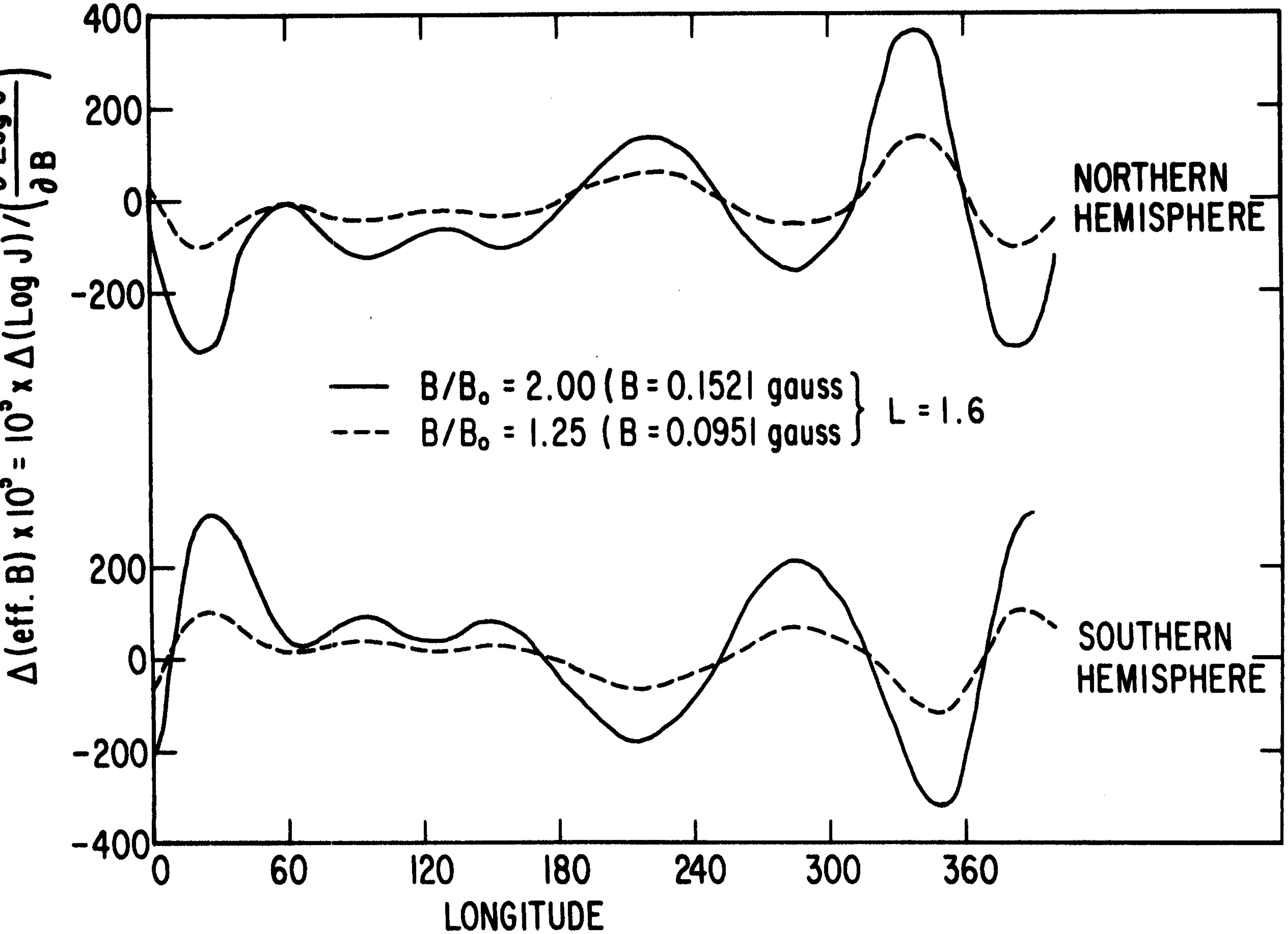

Δ(eff. B) x 10^5 = 10^5 x Δ(Log J)/(∂ Log J / ∂ B)
400
200
0
-200
-400
0
60
120
180
240
300
360
LONGITUDE
B/B₀ = 2.00 (B = 0.1521 gauss)
B/B₀ = 1.25 (B = 0.0951 gauss)
L = 1.6
NORTHERN HEMISPHERE
SOUTHERN HEMISPHERE

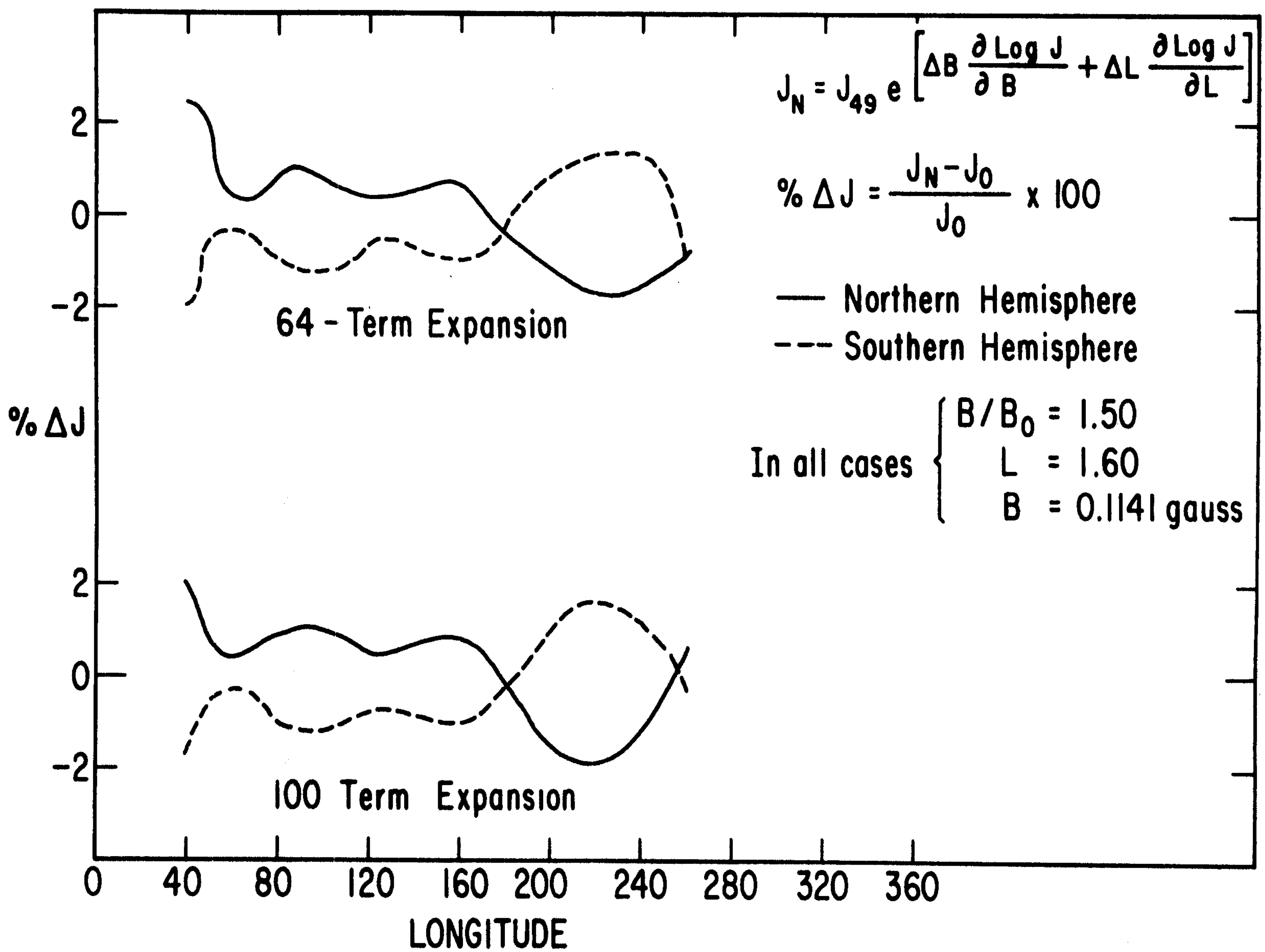

$J_N = J_{49}\, e^{\left[\Delta B \frac{\partial \operatorname{Log} J}{\partial B} + \Delta L \frac{\partial \operatorname{Log} J}{\partial L}\right]}$
$\% \Delta J = \frac{J_N - J_0}{J_0} \times 100$
Northern Hemisphere
Southern Hemisphere
In all cases $B/B_0 = 1.50$, $L = 1.60$, $B = 0.1141$ gauss
64 - Term Expansion
100 Term Expansion
% ΔJ
2
0
-2
0
40
80
120
160
200
240
280
320
360
LONGITUDE

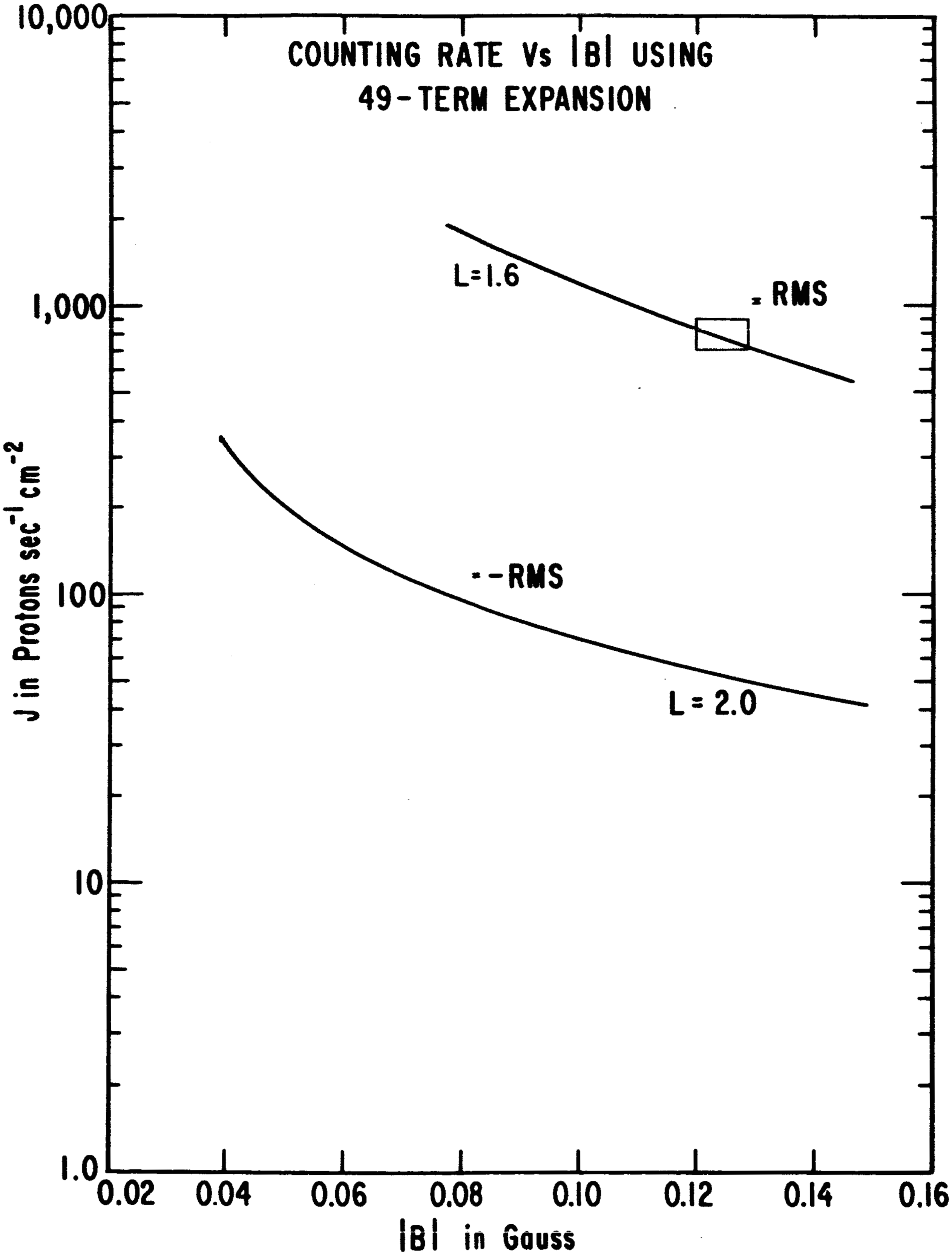

COUNTING RATE Vs |B| USING
49-TERM EXPANSION
L=1.6
RMS
--RMS
L = 2.0
10,000
1,000
100
10
1.0
0.02
0.04
0.06
0.08
0.10
0.12
0.14
0.16
J in Protons sec⁻¹ cm⁻²
|B| in Gauss

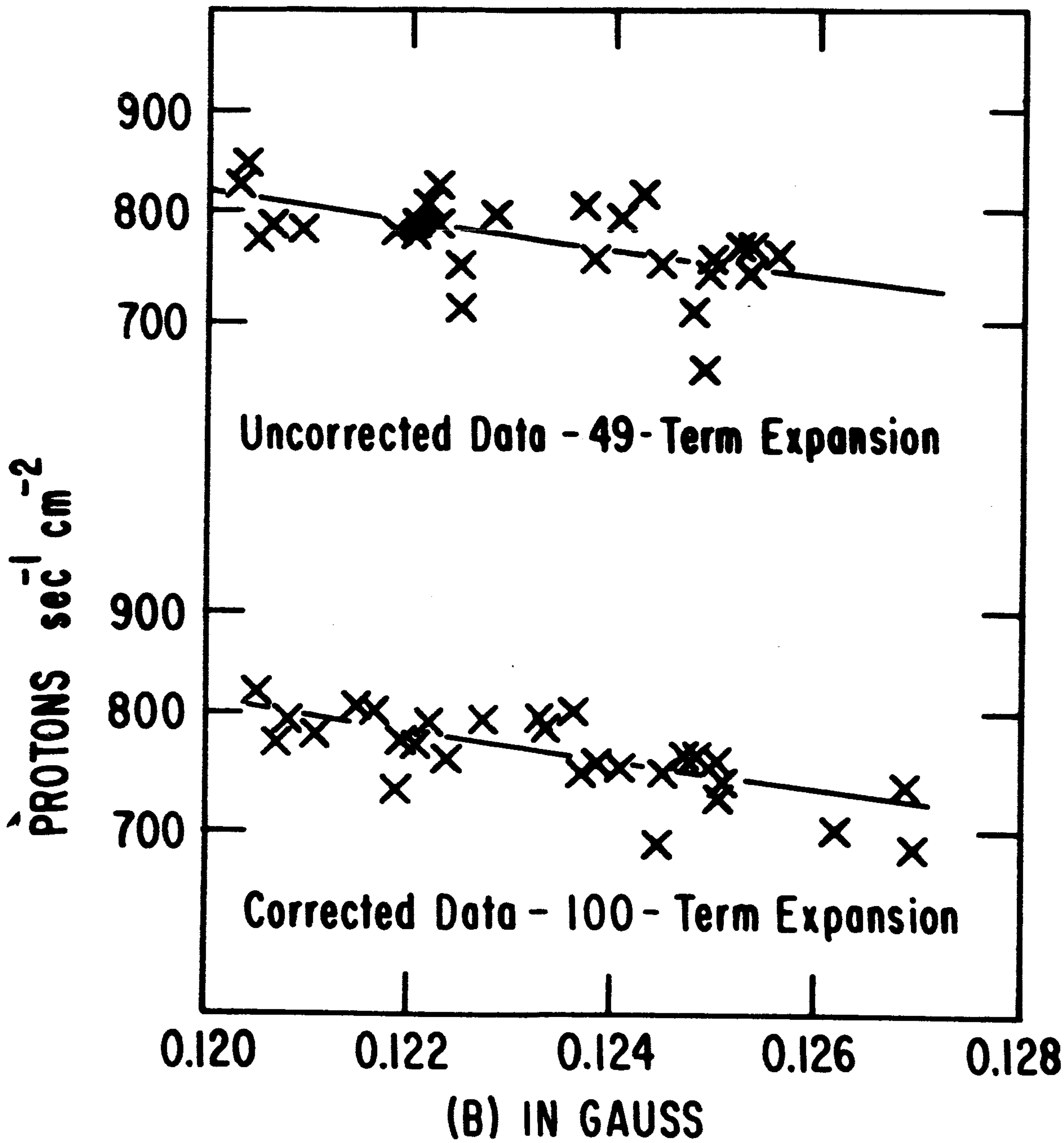

900
800
700
Uncorrected Data - 49 - Term Expansion
PROTONS sec^{-1} cm^{-2}
900
800
700
Corrected Data - 100 - Term Expansion
0.120
0.122
0.124
0.126
0.128
(B) IN GAUSS